

# Suppression of turbulence by mean flows in two-dimensional fluids

Michael SHATS<sup>1</sup>), Hua XIA<sup>1</sup>), Horst PUNZMANN<sup>1</sup>) and Gregory FALKOVICH<sup>2</sup>)

<sup>1</sup>Australian National University, Canberra ACT 0200, Australia

<sup>2</sup>Weizmann Institute of Science, Rehovot 76100, Israel

(Received 15 October 2007)

A review of recent experimental studies of turbulence suppression by mean flows in quasi-two-dimensional fluids is presented. Large-scale mean flows develop during spectral condensation of 2D turbulence as a result of the inverse energy cascade in spatially bounded flow. The spectral energy which is accumulated at the largest scale supports the mean flow which in turn affects turbulence. We show that such a flow can reduce the energy flux in the inverse energy cascade range *via* shearing and sweeping of the turbulent eddies. The former mechanism is more efficient at larger scales, while the latter acts on the smaller scales. Similar suppression of turbulence has been found in the presence of externally imposed flows. Turbulent (inverse energy) cascade is reduced in the presence of imposed flow, but still supports Kolmogorov-Kraichnan  $k^{-5/3}$  power law spectrum in the energy range.

Keywords: two-dimensional fluids, turbulence, mean flow, shear decorrelation, inverse energy cascade

DOI: 10.1585/pfr.1.001

## 1 Introduction

The idea of turbulence suppression in the presence of a background sheared flow has its origin in the physics of magnetically confined plasma. It was proposed in 1990 [1, 2] as a simple hydrodynamic model aimed at explaining turbulence reduction near transport barriers which form in plasma in the so-called high (H) confinement regime [3]. Since then this concept has received wide recognition in the plasma literature (e.g. [4, 5, 6, 7]). The model of the shear suppression is supported by substantial indirect experimental evidence, namely, the correlation between the onset of the strong sheared flows in plasma and the reduction in the turbulent transport during transitions to improved confinement.

The main mechanism of the shear suppression is as follows. When a turbulent eddy is placed in a stable laminar flow whose velocity varies in the direction perpendicular to the flow direction, it becomes stretched and distorted. The shear suppression can be viewed as the reduction in the eddy's lifetime. It occurs when the inverse shearing rate  $\tau_s \approx \omega_s^{-1}$  becomes shorter than the eddy turnover time, or its lifetime,  $\tau_e$  whatever is shorter, providing that the interaction time between turbulence and flow is longer than other time scales. A reduction in the spectral power in the presence of a shear flow is due to the shortened correlation time of eddies. Dimensional scaling analysis which takes into account turbulent diffusion, shows that this shortened correlation time  $\tau_e^s$  is related to the shear straining time  $\tau_s$  and the eddy turnover time  $\tau_e$  as [8]:  $\tau_e^s = \tau_e^{1/3} \tau_s^{2/3}$ . The theory of the shear suppression is considered an extension of the rapid distortion theory into the nonlinear regime [8].

Despite its wide recognition in plasma physics, and attempts to extend its application to other fields (see e.g. [9]), this hydrodynamic phenomenon is not a familiar one in fluids [10]. This fact has triggered arguments both against [11] and in favor [12] of the shear turbulence suppression mechanism, casting a shadow on its existence in plasma.

Results reviewed in this paper represent the first experimental evidence of the turbulence suppression by mean flows in quasi-two-dimensional fluids. First we describe the experimental setup and methods of the turbulent flow detection. Suppression of turbulence is studied (a) during spectral condensation of the spatially bounded flow, and (b) in the presence of externally imposed mean flow.

## 2 Experimental setup and results

In the experiments reported here, turbulent flow is generated in stratified thin layers of electrolyte (NaCl water solutions of different concentrations, heavier solution at the bottom, total thickness of 6 mm). This setup is similar to those used in [13] and [14]. Turbulence is generated by forcing  $576 J \times B$ -driven vortices ( $24 \times 24$ ) in a cell. Spatially varying, vertically directed (normal to the fluid layers) magnetic field  $B$  is produced by a  $24 \times 24$  matrix of permanent magnets placed under the bottom of the fluid cell ( $300 \times 300 \text{ mm}^2$ ) in a checkerboard fashion (10 mm between the centers of magnetic dipoles). The schematic of the experimental setup is shown in Fig. 1. Solid Perspex square boundaries of various sizes are inserted to generate spectral condensate. Two carbon electrodes on the either side of the cell are connected to the power supply. An electric current in the electrolyte can be either modulated, for example, by driving positive and negative current pulses

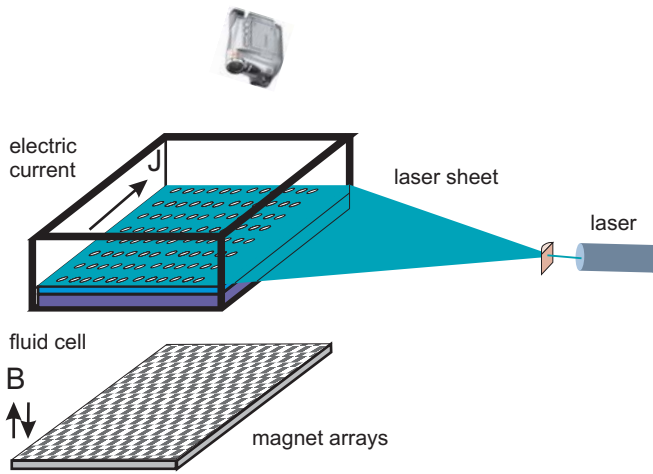


Fig. 1 Schematic of experimental setup.

having random-in-time polarity and the pulse lengths, or it can be DC. Since we are mostly interested in the development of strong coherent condensate flows, a DC mode is chosen in these experiments. Constant forcing is found to be the most efficient in supporting coherent monopole condensate. This agrees with findings of numerical simulations of the generation of large coherent structures in 2D turbulence [15]. The  $J \times B$  forcing is chosen such that there is no ripple on the free surface, which would violate quasi-two-dimensionality of the flow.

To visualize the flow, imaging particles (polyamid, 50  $\mu\text{m}$  diameter, specific gravity of 1.03) are suspended in the top layer of the fluid and are illuminated using thin (1 mm) laser sheet aligned parallel to the free surface of the fluid. Laser light scattered by particles is filmed from above, using video camera at 25 frames per second. Cross-correlation based particle image velocimetry technique is used to obtain the velocity fields from the sequence of the video frames.

First we discuss the generation of the spectral condensate. It is well known that the evolution of spectra in 3D flows leads to the transfer of the spectral energy  $E(k)$ , towards smaller scales (larger  $k$ ), a forward energy cascade, until it reaches the dissipation scale determined by the viscosity. Spectral regions of the turbulence forcing ( $k_f$ ) and of the dissipation range ( $k_d$ ) do not generally coincide. The spectral range between them is called the inertial range. Viscous processes determine the energy dissipation rate  $\epsilon$  in the system. Kolmogorov assumed that (a) the statistical properties of turbulence in the inertial range ( $k \ll k_d$ ) are determined only by  $k$  and  $\epsilon$ , and (b) that  $\epsilon$  is the universal constant of a given flow in time and in space. Dimensional considerations have led to the famous Kolmogorov law for the spectral energy:  $E(k) = C\epsilon^{2/3}k^{-5/3}$ . In 2D flows, in addition to the energy conservation, enstrophy, or the volume integral of the squared vorticity  $\Omega = 1/2 \int \omega^2 dV$  (where  $\omega = \nabla \times V$  is the vorticity and  $V$  is velocity) is also conserved [16]. The existence of this second invariant of the

flow modifies the spectral transfer, which is determined by both the energy and the enstrophy  $\epsilon_\omega$  dissipation rates, and leads to the onset of two inertial ranges. If energy and enstrophy are injected into the system at  $k_f$ , then energy in 2D flow cascades towards larger scales, or lower  $k < k_f$  (inverse energy cascade range), while the enstrophy is transferred towards higher  $k > k_f$  (forward enstrophy cascade). The former is described by the Kolmogorov law,

$$E(k) = C_k \epsilon^{2/3} k^{-5/3}, \quad (1)$$

(though the energy is transferred in the opposite direction to that in the 3D turbulence), while the latter is described by

$$E(k) = C_\omega \epsilon_\omega^{2/3} k^{-3}, \quad (2)$$

The maximum of the energy spectrum thus lies in the low- $k$  range at  $k_E$ , and in the absence of the energy dissipation at large scales  $k_E$  can not be constant in time. In the presence of damping for large scales, for example via linear damping  $\mu$ , the scale corresponding to the maximum of the spectrum, stabilizes at

$$k_E \approx \left( \frac{\mu^3}{\epsilon} \right)^{1/2}. \quad (3)$$

If the system size is larger than this dissipation scale  $\lambda_E = \pi/k_E$ , one should observe the stationary energy spectrum showing two inertial ranges corresponding to the inverse energy cascade ( $\propto k^{-5/3}$ ) and the direct enstrophy cascade ( $\propto k^{-3}$ ). If however dissipative scale is smaller than the system size,  $\lambda_E < L$ , spectral energy is accumulated at the largest scale. Such a process, in which energy piles up in the largest scale  $k_c$ , has been predicted by Kraichnan in 1967 who also noted the similarity between the condensation of the turbulent energy and the Bose-Einstein condensation of the 2D quantum gas [17].

A self-generated coherent flow can develop spontaneously during spectral condensation of the bounded 2D turbulence [17]. In a large domain, inverse cascade proceeds up to the integral scale  $\lambda_E$ . When  $\lambda_E$  is larger than the size of the boundary  $L$ , energy accumulates at the box scale and self-generation of a large vortex occurs. This phenomenon has been confirmed in numerical simulations [18, 19, 20, 21] and has been observed in experiments [22, 13, 14]. For given  $\mu$  and  $\epsilon$ , the easiest way to achieve spectral condensation is to reduce the size of the boundary to satisfy  $\lambda_E \geq L$ . In the described experiments, square boundaries of different sizes of  $L = 90 \div 120$  mm were used. The spectral condensation leads to the onset of the self-generated mean flow, which interacts with the background turbulence.

First we consider the effect of the self-generated flow on the bounded ( $L = 110$  mm) turbulence [23]. The time evolution of the total kinetic energy of the 2D turbulent flow is shown in Fig. 2(a). The inverse energy cascade leads to the development of larger eddies and to the growth

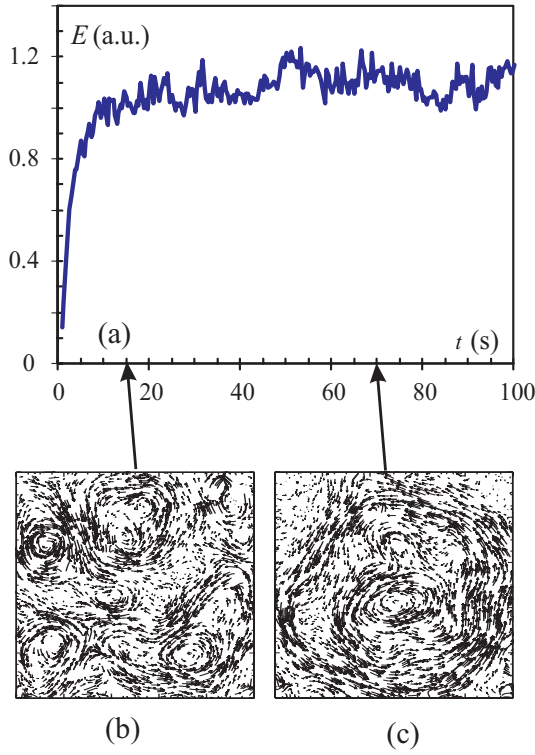


Fig. 2 Time evolution of the total kinetic energy (a) and instantaneous velocity fields at  $t = 13$  s (b), and  $t = 71$  s (c).

of the kinetic energy of the system. By about 10 s the kinetic energy reaches 80% of its maximum value. By this time several large-scale coherent vortices develop in the flow, as seen in Fig. 2(b). These vortices persist for 4-5 turnover times (about 10 s) before they start merging. After this transient stage, large vortices merge to form a single coherent vortex, which then persists in a steady state, Fig. 2(c). This stable vortex imposes mean flow which affects 2D turbulence.

We compare the turbulence spectra during the transient stage, at  $t = (9 - 17)$  s, and after the single vortex formation, at  $t = (61 - 79)$  s. The analysis time in the transient stage is limited to 8 s during which the flow is quasi-steady. The wave number spectra are averaged over  $N = 200$  realizations (400 in the steady condensate regime) of the “instantaneous” velocity fields (computed every 40 ms using two consecutive video frames):

$$E_{tot}(k) = 1/N \sum_{n=1}^N F(V)F^*(V), \quad (4)$$

where  $F$  denotes Fourier transform and  $F^*$  is its complex conjugate. This is a total spectrum which includes both mean and fluctuating velocity. Before the large vortex formation, this spectrum shows a power-law scaling of  $E(k) \propto k^{-3}$  both above and below the forcing wave number  $k_f = 350 \text{ m}^{-1}$ , Fig. 3(a). Such a scaling, which was already observed in the experiments in the spectral condensate regime [14] and in numerical simulations [24, 25, 26, 21], apparently contradicts the  $E(k) \propto k^{-5/3}$  spectrum expected for

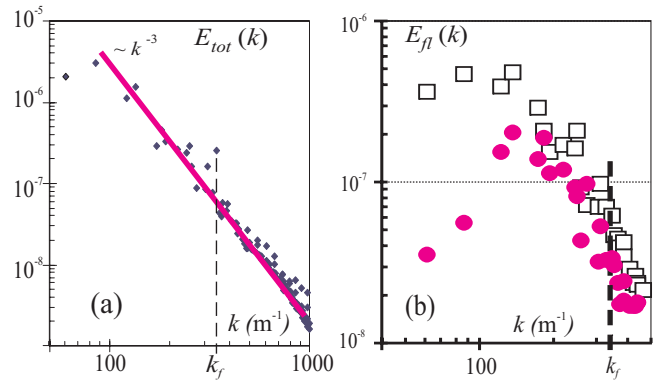


Fig. 3 Spectrum of the total spectral energy of the flow at  $t = (9-17)$ s (a). Spectra of the turbulent velocity fluctuations before,  $t = (9-17)$ s (open squares) and after the formation of a single large vortex,  $t = (61-79)$ s (solid circles) (b).

the inverse energy cascade inertial range [17]. It was suggested in [21] that a  $k^{-3}$  power law is due to the presence of large-scale persistent vortices rather than due to the turbulent cascade. To eliminate this effect, we subtract from the instantaneous velocity the mean  $\langle V \rangle = 1/N \sum_{n=1}^N V(x, y)$  obtained by averaging over  $N$  instantaneous fields  $V(x, y)$ . The resulting spectra,

$$E_{fi}(k) = 1/N \sum_{n=1}^N F(V - \langle V \rangle)F^*(V - \langle V \rangle), \quad (5)$$

computed for two time intervals, before and after the generation of the single vortex, are shown in Fig. 3(b). Such subtraction, proposed in [21], leads to a spectrum less steep than  $k^{-3}$ , somewhat close to  $k^{-5/3}$ .

After the formation of the single vortex, turbulence levels are significantly reduced for the wave numbers in the range of  $k < 160 \text{ m}^{-1}$ . The explanation of this will be given below. The level of turbulent fluctuations changes less between  $k \approx 160 \text{ m}^{-1}$  and the injection scale,  $k_f \approx 350 \text{ m}^{-1}$ . That interval is too short to distinguish between  $E_{fi}(k) \propto \epsilon^{2/3}k^{-5/3}$  and  $E_{fi}(k) \propto \epsilon/\tau_s k$  that one may expect assuming that the scale-independent energy transfer is of order of the shear time  $\tau_s$ . One can see that in the forward cascade range ( $k \geq k_f$ ) fluctuations are also reduced. This reduction at small  $k$  is significant (up to a factor of ten) and reproducible.

Now we turn to the experiment in which a large-scale mean flow was externally imposed on the quasi-2D turbulence [23]. The flow is generated using large permanent magnet, as illustrated in Fig. 4. In this case the boundary box exceeds the integral scale ( $L \approx 300 \text{ mm}$ ). We refer to this configuration as to “unbounded” turbulence.

A large magnet ( $40 \times 40 \text{ mm}^2$ ) placed 2 mm above the free surface imposes a large-scale vortex flow, which slowly decays (for approximately 60 seconds) after the magnet is removed. Instantaneous velocity fields before and after the generation of this mean flow are shown in Figs. 5(a,b). Energy spectra shown in Figs. 5(c) are com-

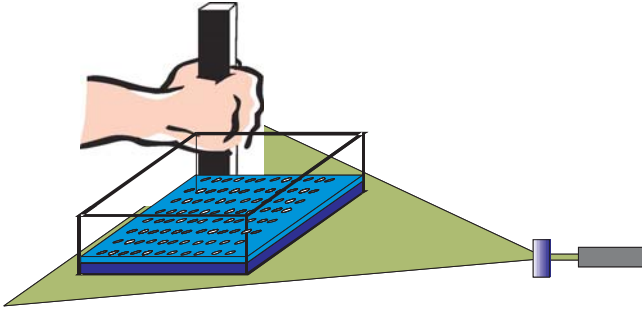


Fig. 4 Schematic of the generation of external mean flow

puted after subtracting the mean flow, using Eq. 5. Both with and without the large vortex, spectra are close to the  $k^{-5/3}$  scaling. The mean flow reduces the spectral power of the turbulent fluctuations everywhere within the inverse cascade range by a factor of 8.

### 3 Analysis and discussion

In the presence of the self-generated large vortex the observed reduction in the spectral power of turbulent eddies is consistent with the mechanism of the shear turbulence suppression. We estimate the shear suppression criterion  $s = \omega_s \tau_e > 1$  as follows. The turnover time of an eddy of the scale  $l$  is

$$\tau_e \approx \frac{l}{\langle |\delta V(l)| \rangle} = \frac{l}{S_1(l)}, \quad (6)$$

that is estimated from the mean velocity difference across scale  $l$ ,

$$\delta V(l) = V(r_0 + l) - V(r_0). \quad (7)$$

The angular brackets denote averaging over all possible positions  $r_0$  within the boundary box (or within the computation box in the “unbounded” case), and  $S_1 = \langle \delta V \rangle$  is the first-order structure function averaged over  $N$  velocity fields.

To estimate the shearing rate of the large-scale mean flows, both self-generated [Fig. 2(c)] and externally forced [Fig. 5(b)], the polar coordinate system with its origin in the center of the vortex is used. The azimuthal component of the velocity  $V_\theta$  dominates the flow after the vortex is formed. Its radial distribution is shown in Figs. 6(a,c). In the case of the self-generated flow radial coordinates  $r = 0$  and  $r = 0.05$  m correspond to the vortex center and to the square boundary respectively. In the case of externally driven flow  $r = 0.09$  m corresponds to the size of the imaged area of “unbounded” turbulent flow. It is seen that the amplitude of velocity of the externally forced flow is a factor of two higher than in the self-organized case. The shearing rate is determined as follows:

$$\omega_s = l \frac{d\Omega}{dr}, \quad (8)$$

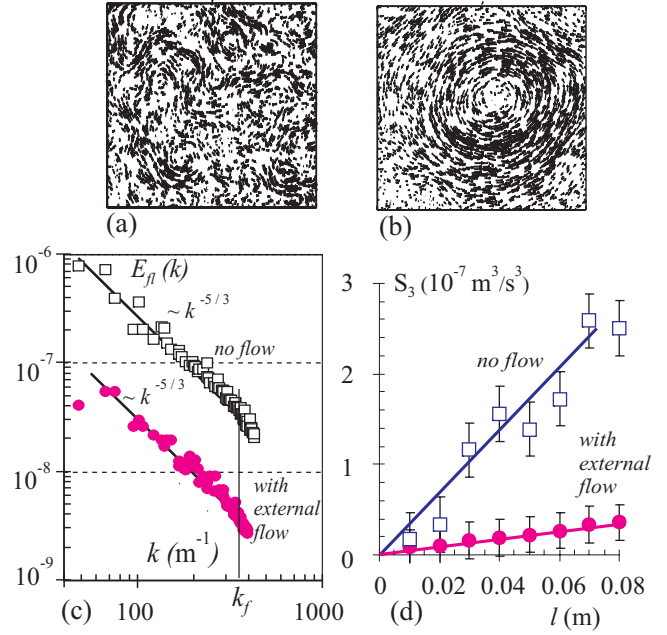


Fig. 5 Instantaneous velocity fields of “unbounded” turbulence (a) and in the presence of externally generated large scale azimuthal flow. Spectra of turbulence are computed with mean flow subtracted: before the large flow is imposed (open squares) and in the presence of the mean flow (solid circles). Third-order structure functions without (open squares) and with (solid circles) externally imposed mean flow (d).

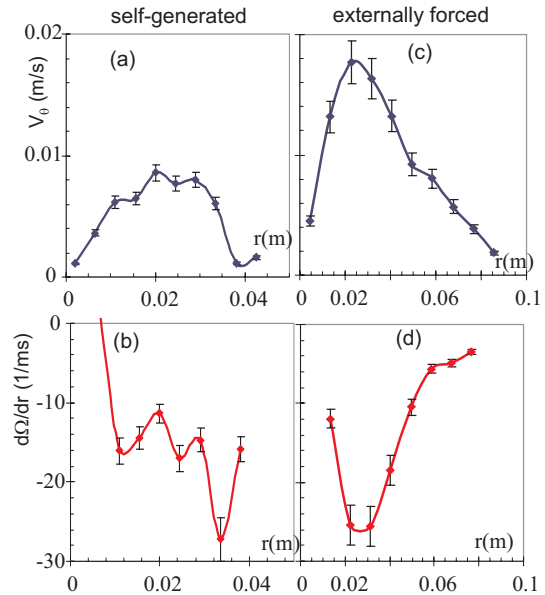


Fig. 6 Mean azimuthal velocity of the flow after the large-scale vortex generation (a,c) and the derivative of its angular velocity (b,d) during spectral condensation of the bounded turbulence (a,b), and in the case of externally forced “unbounded” flow (c,d).

where  $l$  is the radial extent of the eddy. The derivative of the radially localized angular velocity  $\Omega = V_\theta/r$  is determined as

$$\frac{d\Omega}{dr} = \frac{1}{r} \frac{dV_\theta}{dr} - \frac{V_\theta}{r^2}, \quad (9)$$

which is zero for the solid-body mean flow rotation and nonzero for the sheared flow. Figs. 6(b,d) show  $d\Omega/dr$  for the self-generated and externally driven shear flows. Since both  $\omega_s$  and  $\tau_e$  grow with  $l$ , the shear affects larger scales first.

For the case of the self-generated flow  $d\Omega/dr \approx 15 (ms)^{-1}$ ,  $S_1 \approx 8 \times 10^{-3}$  m/s, and the shearing parameter  $s \approx 2 \times 10^3 l^2$ . The criterion for the shear suppression,  $s > 1$ , is satisfied for the scales  $l > 0.022$  m. This gives an estimate of the affected wave number range  $k = \pi/l \leq 145 m^{-1}$ , which is in agreement with the observation of the turbulence suppression in the wave number range of  $k \leq 160 m^{-1}$  seen in Fig. 3(b).

For the externally forced mean flow  $d\Omega/dr \approx 22 (ms)^{-1}$ ,  $S_1 \approx 2 \times 10^{-3}$  m/s, and the shearing parameter  $s \approx 1.1 \times 10^4 l^2$ . The suppression criterion is satisfied for the scales  $l > 0.0095$  m, which extends very close to the forcing scale  $l_f \approx 9$  mm ( $k_f = 350 m^{-1}$ ). Again, this is in agreement with our observation that the spectral energy is reduced everywhere within the inverse energy cascade inertial range, Fig. 5(c).

The externally driven flow must be strong enough to affect the energy flux through the  $k < k_f$  inertial range. To test this we computed the third-order structure function  $S_3(l) = \langle \delta V(l)^3 \rangle$  to estimate the energy flux  $\epsilon$  from the Kolmogorov law,

$$S_3(l) = -\frac{3}{2} \epsilon l. \quad (10)$$

Similarly to  $S_1$ , the third-order structure function  $S_3$  is computed by averaging over the boundary box and then by averaging  $S_3$  in time over 100 subsequent velocity fields. It should be noted that  $\delta V(l)$  represents here the longitudinal velocity increment,  $\delta V_{||}(l)$ , defined in Kolmogorov's theory [16]. Also,  $S_3$  is computed allowing positive and negative values of the velocity increments  $\delta V_{||}(l)$ . Such computations require very large statistical averaging to obtain converged results. We obtained satisfactory convergence for the steady-state "unbounded" turbulence and for the turbulence in the presence of the slowly decaying externally driven flow. The result is illustrated in Fig. 5(d). Both before and after the mean flow is imposed,  $S_3$  is a linear function of the scale  $l$ . As a result, the energy flux  $\epsilon = -(2/3)S_3/l$  is constant to within 15% for all scales in the energy inertial range. This flux  $\epsilon$  is reduced in the presence of the flow by one order of magnitude compared to the case without the flow.

The reduction in the energy flux can be attributed to two phenomena in this case. First, it is the shearing of the forcing scale vortices discussed above. However, the

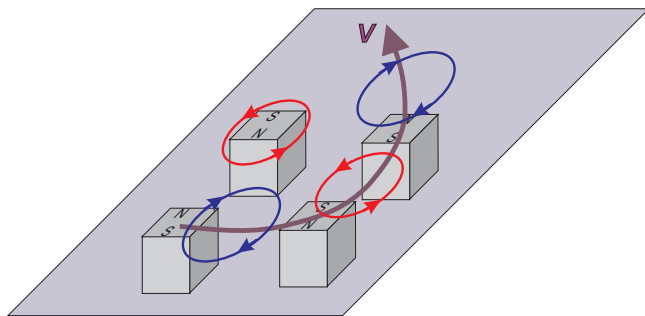


Fig. 7 Schematic illustration of the effect of sweeping of the forcing scale vortices by mean flow relative to the magnets

force-connected vortices (with  $k \approx k_f$ ) must be more resistant to shearing than the inertial scale eddies at  $k < k_f$ . Second, the force-fed vortices are *swept* by the mean flow relative to the magnets, which must also reduce the energy input. This effect is schematically illustrated in Fig. 7.

One can define a dimensionless sweeping parameter  $sw = \omega_{sw} \tau_e$ , where the sweeping rate is given by  $\omega_{sw} = V_\theta/l$ . Since

$$sw = \frac{V_\theta}{l} \frac{l}{S_1} \sim V_\theta(\epsilon l)^{-1/3}, \quad (11)$$

sweeping acts more efficiently on the smaller scales (while shearing is more effective on larger scales). At the forcing scale  $l_f$ , this parameter is  $sw \approx 0.75$  for the self-generated flow and it is  $sw \approx 7$  with externally forced mean flow. Thus the sweeping can be responsible for the reduction in the energy flux through the inverse cascade range in the presence of an externally-induced flow. The dominant role of sweeping in this case is also supported by the fact that the spectrum of the inverse cascade remains  $k^{-5/3}$ , just shifted down as shown in Fig. 5(c). Such modifications to the spectrum are also consistent with a ten-fold decrease in the energy flux  $\epsilon$ , since  $E(k) = C_k \epsilon^{2/3} k^{-5/3}$ .

Let us stress the qualitative difference between Fig. 3(b) (strong decrease at small  $k$ ) and Fig. 5(c) (uniform decrease for all  $k$ ) which shows that there are two mechanisms of suppression. Sweeping may also be responsible for the reduction in the enstrophy flux through the forward cascade ( $k > k_f$ ) in the presence of the self-generated flow [see Fig. 3(b)]. In this case, we could not obtain statistically converged computations of  $S_3$  during spectral condensation to compare  $\epsilon$  before and after the formation of the large vortex.

## 4 Conclusions

We have shown in [23] that turbulence is quasi-2D flow is significantly reduced in the presence of a large coherent vortex. In the case of a self-generated vortex, larger scales are affected more than the smaller ones. This qualitatively

agrees with the description of the shear turbulence suppression mechanism as a reduction in the eddy life-time [1]. In the presence of externally imposed flow two effects may be responsible for the observed strong reduction in the turbulence level. The vortex sweeping by the mean flow seems to play an important role here. In this case the shape of the spectrum is not modified but the (inverse) spectral energy flux is substantially reduced.

It should be noted that three conditions needed for the shear turbulence suppression in fluids discussed in [10] are satisfied in our experiment. The shear flow must be stable in a sense that the time during which turbulence remains in the region of flow shear should exceed both the eddy life-time  $\tau_e$  and the shear straining time  $\tau_s$ . The shear flow is stable in our experiment. Due to the dominant flow in the azimuthal direction after the monopole formation, turbulence stays in the region of shear,  $\rho = (0.2 - 0.9)$ , Fig. 6. Finally, the 2D dynamics of the flow is imposed on the system by the stratification of thin fluid layers.

The mechanism of the shear suppression in plasma is often described as the loss of coherence by a turbulent eddy and a breakup into two eddies of the smaller scale (e.g. [9]). One would expect in this case an increase in the spectral power of eddies of intermediate scales. We have not found any evidence in support of the eddy breakup. Observations in 2D fluids are more consistent with the idea of reduction in the turnover time of the larger scale eddies [8]. In this case the inverse energy cascade is arrested at the scales affected by the shear flow, which presumably leads to the reduction in the spectral energy, similar to that seen in Fig. 3(b).

- [1] H. Biglari, P.H. Diamond and P.W. Terry, *Phys. Fluids B* **2** (1990) 1.
- [2] K.C. Shaing, E.J. Crume and W.A. Houlberg, *Phys. Fluids B* **2** (1990) 1492.
- [3] F. Wagner et al. *Phys. Rev. Lett.* **49** (1982) 1408.
- [4] T.S. Hahm and K.H. Burrell, *Phys. Plasmas* **2** (1995) 1648.
- [5] T.S. Hahm, *Phys. Plasmas* **4** (1997) 4074.
- [6] K.H. Burrell, *Phys. Plasmas* **6** (1999) 4418.
- [7] K.H. Burrell, *Phys. Plasmas* **4** (1997) 1499.
- [8] P.W. Terry, *Rev. Mod. Phys.* **72** (2000) 109.
- [9] E.-J. Kim, *Astron. and Astrophysics* **441** (2005) 763.
- [10] P.W. Terry, *Phys. Plasmas* **7** (2000) 1653.
- [11] D.C. Montgomery, *Phys. Plasmas* **7** (2000) 4785.
- [12] P.W. Terry, *Phys. Plasmas* **7** (2000) 4787.
- [13] J. Paret and P. Tabeling, *Phys. Fluids* **10** (1998) 3126.
- [14] M.G. Shats, H. Xia, H. Punzmann, *Phys. Rev. E* **71** (2005) 046409.
- [15] N.N. Kukharkin, *J. Sci. Comp.* **10** (1995) 409.
- [16] U. Frisch, *Turbulence: The Legacy of A. N. Kolmogorov* (Cambridge University Press, Cambridge, 1995).
- [17] R.H. Kraichnan, *Phys. Fluids* **10** (1967) 1417.
- [18] M. Hossain, W. H. Matthaeu, D. Montgomery, *J. Plasma Phys.* **30** (1983) 479.
- [19] L. M. Smith, V. Yakhot, *Phys. Rev. Lett.* **71** (1993) 352.
- [20] D. Molenaar, H.J.H. Clercx and G.J.F. van Heijst, *Physica D* **196** (2004) 329.
- [21] M. Chertkov, C. Connaughton, I. Kolokolov and V. Lebedev, *Phys. Rev. Lett.* **99** 084501 (2007).
- [22] J. Sommeria, *J. Fluid Mech.* **170** (1986) 139.
- [23] M.G. Shats, H. Xia, H. Punzmann and G. Falkovich *Phys. Rev. Lett.* **99** 164502 (2007).
- [24] V. Borue, *Phys. Rev. Lett.* **72** (1994) 1475.
- [25] L.M. Smith and F. Waleffe, *Phys. Fluids* **11** (1999) 1608.
- [26] C. V. Tran and J. C. Bowman, *Phys. Rev. E* **69** (2004) 036303.